Dark States in Monomeric Red Fluorescent Proteins Studied by Fluorescence Correlation and Single Molecule Spectroscopy

Jelle Hendrix,* Cristina Flors,† Peter Dedecker,† Johan Hofkens,† and Yves Engelborghs*
*Laboratory of Biomolecular Dynamics, Department of Chemistry, Katholieke Universiteit Leuven, 3001 Heverlee, Belgium; and †Laboratory of Photochemistry and Spectroscopy and Institute for Nanoscale Physics and Chemistry, Department of Chemistry, Katholieke Universiteit Leuven, 3001 Heverlee, Belgium

ABSTRACT Monomeric red fluorescent proteins (mRFPs) have become indispensable tools for studying protein dynamics, interactions and functions in the cellular environment. Their emission spectrum can be well separated from other fluorescent proteins, and their monomeric structure preserves the natural function of fusion proteins. However, previous photophysical studies of some RFPs have shown the presence of light-induced dark states that can complicate the interpretation of cellular experiments. In this article, we extend these studies to mRFP1, mCherry, and mStrawberry by means of fluorescence correlation spectroscopy and prove that this light-driven intensity flickering also occurs in these proteins. Furthermore, we show that the flickering in these proteins is pH-dependent. Single molecule spectroscopy revealed reversible transitions from a bright to a dark state in several timescales, even up to seconds. Time-resolved fluorescence spectroscopy showed multiexponential decays, consistent with a "loose" conformation. We offer a structural basis for the fluorescence flickering using known crystal structures and point out that the environment of Glu-215 is critical for the pH dependence of the flickering in RFPs. We apply dual-color fluorescence correlation spectroscopy inside live cells to prove that this flickering can seriously hamper cellular measurements if the timescales of the flickering and diffusion are not well separated.

INTRODUCTION

The green fluorescent protein (GFP) was discovered in 1961 in the hydrozoan *Aequorea victoria* (1). Fluorescence microscopy in live cells has been revolutionized since the advent of the GFP as a genetically encoded marker in 1992 (2). In the following years, variants of the GFP with different absorption/emission maxima and higher brightness and stability have created a fluorescence palette ranging from blue (eBFP) to yellow (eYFP, Citrine). In 1999, this palette was extended to the red by the discovery of red fluorescent proteins (RFPs) in anthozoans like *Discosoma* sp. (DsRed) and in 2002 also in *Entacmaea quadricolor* (eqFP611) (3,4).

Being an obligate tetramer, DsRed was engineered in 2002 by Campbell et al. into mRFP1, the first true monomeric red fluorescent protein (5). mRFP1 contains 33 amino acid mutations but is structurally still very stable (6). The chromophore in mRFP1 matures much faster than in DsRed, it is less bright, and its photostability is lower than DsRed but still comparable to eGFP (5).

In 2004, further engineering of mRFP1 led to the mFruits family that covers the yellow (mHoneydew) to dark-red part (mPlum) of the visible spectrum (7,8). Of the mFruits, mCherry is considered to be the superior monomeric RFP (9). It has a good photostability and even faster maturation but still is only moderately brighter than mRFP1. A brighter version of mRFP1 exists (Q66T), but at the cost of a 34-nm blue shift of the emission spectrum (10). Recently, a new mRFP (TagRFP) has been created from eqFP578, but the emission spectrum still is 24-nm blue-shifted with respect to mRFP1 (11). mRFP1 has also been converted into a photoactivatable protein (12).

mRFPs are in great demand for experiments in live cells because of their interesting properties. First, their red emission leads to less scattering and less background fluorescence detection. Second, their emission spectrum can be well separated from eGFP, which makes them interesting for dual color applications. Moreover, when fused to a certain protein, their monomeric structure preserves the natural function and allows for Förster resonance energy transfer measurements. However, previous photophysical studies of some RFPs have shown the presence of light-induced dark states that can complicate the interpretation of the results of the cellular measurements (13–15).

In 2000, Heikal et al. observed with fluorescence correlation spectroscopy (FCS) that DsRed in solution shows a large contribution of an excitation intensity-dependent (but not pH-dependent) flickering in the submillisecond timescale (13). Subsequently, Malvezzi-Campeggi et al. proved that this flickering represents the transition between three interconvertible states (a red, a far-red, and a dark state) (14). Schenk et al. confirmed the observations for DsRed and observed a similar process in a different RFP, eqFP611 (15). The flickering was suggested to be a consequence of conformational rearrangements around the chromophore, such as photoisomerization and/or changes in the hydrogen-bonding network. Both for DsRed and eqFP611, Raman spectroscopy later showed that photoisomerization is indeed involved in the photodynamics of these RFPs (16,17). In some GFP

Submitted October 9, 2007, and accepted for publication December 21, 2007.

Address reprint requests to Yves Engelborghs, E-mail: yves.engelborghs@fys.kuleuven.be.

Editor: Enrico Gratton.

0006-3495/08/05/4103/11 $2.00

doi: 10.1529/biophysj.107.123596

mutants such as eYFP and Citrine (13,18), a pH- and intensity-dependent flickering was also found and assigned to fast protonation-deprotonation.

In this article, we focus on the monomeric red fluorescent proteins mRFP1, mStrawberry, and mCherry and on the presence of light-induced flickering. We have characterized this process with fluorescence correlation and single-molecule spectroscopy, and we have explored the effects of viscosity, excitation intensity, and pH on this process. We have combined our experimental results with information based onknown x-ray structures of some RFPs, and we provide insight into the consequences that the chromophore environment has on the observed fluorescence properties. Also, we draw the attention to the implications of the fast flickering of RFPs when performing quantitative FCS measurements in live cells.

MATERIALS AND METHODS

Proteins and buffers

The pRSET plasmids coding for His-tagged mRFP1, mCherry, and mStrawberry were a kind gift of Dr. Roger Y. Tsien (Howard Hughes Medical Institute-University of California at San Diego, La Jolla, CA). After transformation of the plasmid in *E. coli* BL21 cells, the cells were grown at 37°C to an optical density of 0.6 after which protein overexpression was induced during 3 h with 1 mM IPTG. After sonication of the culture, the proteins were purified using gravity flow Ni^{2+}-affinity chromatography (Protino Ni-TED, Macherey-Nagel GmbH & Co. KG, Düren, Germany). The protein purity was checked with sodium dodecyl-sulfate-polyacrylamide gel electrophoresis. On this gel, three bands could be observed, corresponding to native and cleaved protein. The cleavage occurs in the chromophore and is caused by a partial hydrolysis of the main chain acylimine linkage ((5,12,19) and data not shown). The extent of the cleavage does not increase over time, suggesting that the cleavage occurs only in a subpopulation, which may represent poorly folded protein. This suggestion is underpinned by the fact that a larger extent of cleavage occurs in the photoactivatible PA-mRFP1-1 than in mRFP1 (20), which might be due to the mutations in the chromophore environment. The cleavage irreversibly changes the spectral properties of the RFP, converting it from a red to a green-like protein. The residual fluorescence of the green-like protein, if any, will not influence our measurements, because we are using a red emission filter.

Most of the experiments were performed in phosphate buffered saline (PBS, pH 7.4). The pH buffer consisted of 50 mM of phosphate, citrate, and glycine adjusted from pH 3–12 (with 0.5 increments) with 3 N of NaOH. If a higher viscosity was needed, glycerol was added to the buffer, and the pH was adjusted with NaOH containing the same concentration of glycerol.

Samples for single-molecule measurements were prepared by spin-coating the proteins ($\sim 10^{-11}$ M) in PBS containing 1% (wt) polyvinyl alcohol (PVA) on a clean cover glass at 3000 rpm.

Absorption and emission spectra

Absorption spectra were measured with a Shimadzu UV-1601PC spectrophotometer (Shimadzu GmbH, Duisburg, Germany). Excitation and emission spectra were taken with a PTI QuantaMaster fluorometer (Photon Technologies International, West Sussex, UK). For the excitation spectra, the excitation monochromator bandwidth was set to 2 nm, and the emission monochromator was set to 650 ± 10 nm. For the emission spectra, the excitation monochromator was set to 540 ± 10 nm, and the emission monochromator bandwidth was set to 2 nm.

FCS in solution

For FCS measurements in solution, the concentrated protein was diluted to 1 nM in the appropriate buffer. The measurements were performed on a commercial ConfoCor2 system (Carl Zeiss, Jena, Germany). A 543-nm HeNe laser was used to excite mRFP1, with the acousto-optical tunable filter set to 3%–100%, corresponding to an intensity of 2–122 kW/cm^2 in the confocal spot (as measured with a light power meter). The excitation light was reflected by a HFT543 dichroic mirror and focused in the sample through a C-Apochromat 40×/1.2NA water immersion objective. The fluorescence light was filtered by a LP560 longpass filter and was detected on an avalanche photodiode through a 78-μm pinhole. For the different experimental conditions (e.g., intensity and pH), 10 measurements of 20-s duration each were performed, and the average autocorrelation curve was calculated. The measurements were analyzed in Igor Pro 5 (Wavemetrics, Portland, OR) by means of global analysis. The model used to fit the curves has the following general form:

$$G(\tau) = G_{\mathrm{T}}(\tau) \times G_{\mathrm{D}}(\tau)$$
$$G_{\mathrm{T}}(\tau) = \prod_{x=1}^{n}\left(1 + \frac{F_x e^{-\tau/\tau_x}}{1 - F_x}\right)$$
$$G_{\mathrm{D}}(\tau) = \frac{1}{\langle N\rangle}\left(1 + \frac{4D\tau}{\omega_1^2}\right)^{-1}\left(1 + \frac{4D\tau}{\omega_2^2}\right)^{-1/2}, \qquad (1)$$

with G_{T} the part of the autocorrelation curve at a fast timescale, representing the photodynamics; G_{D} the concentration dependent part at slower timescale, representing diffusion; τ the correlation time; F_x and τ_x the fraction and time of the fast process; n the total number of fast processes; $\langle N\rangle$ the average number of particles in the confocal volume element; D the apparent diffusion coefficient; and ω_1 and ω_2, respectively, the radial and axial radii of the confocal volume element, which are determined by a calibration with Rhodamine 6G and are fixed throughout the fitting routine.

Single-molecule fluorescence spectroscopy and ensemble time-resolved fluorescence

For single-molecule experiments, excitation at 543 nm (8 MHz, 1.2 ps full width at half-maximum) from the frequency doubled output of an optical parametric oscillator (GWU Lasertechnik, Erftstadt-Friesheim, Germany) pumped by a Ti:Sapphire laser (Tsunami, Spectra Physics, Utrecht, The Netherlands) was directed into an inverted microscope (IX 70, Olympus Optical, Tokyo, Japan) and focused onto the sample through an oil immersion objective (60×/1.4NA, Olympus). Fluorescence was collected through the same objective and sent to an avalanche photodiode (SPCM-AQR-15, PerkinElmer, Waltham, MA). For the single-molecule experiments, the excitation intensity was 120 nW, which corresponds to ~261 W/cm^2. Time-resolved data were collected with a time-correlated single photon counting (TCSPC) card (SPC 630, Becker & Hickl GmbH, Berlin, Germany) operated in first-in-first-out mode. The detailed description of the setup and the data acquisition process has been published previously (21).

Ensemble time-resolved fluorescence measurements were performed using the TCSPC technique (22), with excitation at 543 nm and using the same source as above, in a cuvette with a path length of 1 cm and an optical density of 0.1 at the absorption maximum. Fluorescence was detected under magic angle geometry by means of a cooled microchannel plate photomultiplier (Hamamatsu R3809U (Hamamatsu City, Japan)). Fluorescence histograms of the sample and of the instrument response function were collected in 4096 channels until they typically reached 10^4 counts in the peak channel. The total width at half-maximum of the instrument response function was ~40 ps.

RESULTS

Fluorescence correlation spectroscopy of mRFP1 and mFruits

We applied FCS to discover if dark-state formation also occurs in mRFP1, mCherry, and mStrawberry, as found for the other RFPs described in the Introduction. As the viscosity of the medium only affects the translational diffusion, we can exploit it for the identification of nondiffusion-related processes. Whereas at 24 kW/cm^2 in aqueous buffer there are no distinct components visible in the autocorrelation curve (Fig. 1, *left curve*), in 50% (v/v) glycerol two different components are clearly visible (Fig. 1, *right curve*). The fastest component can be adequately described by an exponential blinking term in the fitting function, and the slowest is best described by a translational diffusion term. The relaxation time of the fast component is much faster than the expected time necessary for a typical monomeric GFP to diffuse through the confocal volume, confirming its identity as a nondiffusion-related process. The fraction of flickering for mRFP1 and for mCherry molecules at 24 kW/cm^2 is similar, 46% ± 1% and 43% ± 2%, respectively. At the same I_{exc}, mStrawberry showed a markedly increased fraction, 56% ± 1%. Furthermore, the flickering also experienced a small viscosity effect. It should be noted, however, that glycerol changes the refractive index of the solution, which also has an effect on the autocorrelation curve (23). Nevertheless, this experiment proves that also in these mRFPs dark-state formation occurs in a timescale of tens of microseconds.

Intensity dependence

To determine if the dark-state formation is light-induced, we performed FCS measurements at different excitation intensities ranging from 2 to 122 kW/cm^2 (Fig. 2 *A*). First, we determined the diffusion coefficient of mRFP1 in aqueous solution. The brightness of mRFP1 was not linearly dependent on I_{exc} at high excitation intensity (data not shown), which can be attributed to optical saturation of the fluorescent protein (23). This optical saturation in combination with a larger contribution of flickering processes at higher I_{exc} caused the apparent D to vary with I_{exc}. By measuring at varying I_{exc} and extrapolating to $I_{exc} = 0$ (Fig. 2 *B*), we obtained a value of $D = \sim 56\ \mu m^2/s$, which is in good agreement with the value found for eGFP. Two-focus FCS might provide a confirmation for the value we obtained because, in this technique, D is measured relative from one focus to another and so is less prone to optical artifacts (24).

Fig. 2, *C* and *D*, show, respectively, the relaxation time and the fraction of the nondiffusion-related process(es). In the low I_{exc} regime, the fraction and relaxation time of the flickering are clearly light-dependent (*squares* in Fig. 2, *C* and *D*), meaning that the path toward the dark state is favored, i.e., the dark state formation is indeed light-induced. In the higher I_{exc} regime, the fraction of the flickering appears to become constant. In addition, a second exponential term had to be included in the fitting. As an illustration, a fit of the FCS curve at the highest I_{exc} with one exponential function is also shown in Fig. 2 *A*. The relaxation time of the second exponential term could be kept constant, and the fraction showed a linear increase (*circles* in Fig. 2, *C* and *D*) even in the region where the other process appeared to have become saturated. This second process might represent another light-induced state, e.g., triplet conversion (25,26). Triplet lifetimes of RFPs such as HcRed have been estimated at a few microseconds (27), a finding similar to our observations. Due to the low triplet quantum yield in GFPs (28), the exponential term that accounts for its formation only becomes apparent at

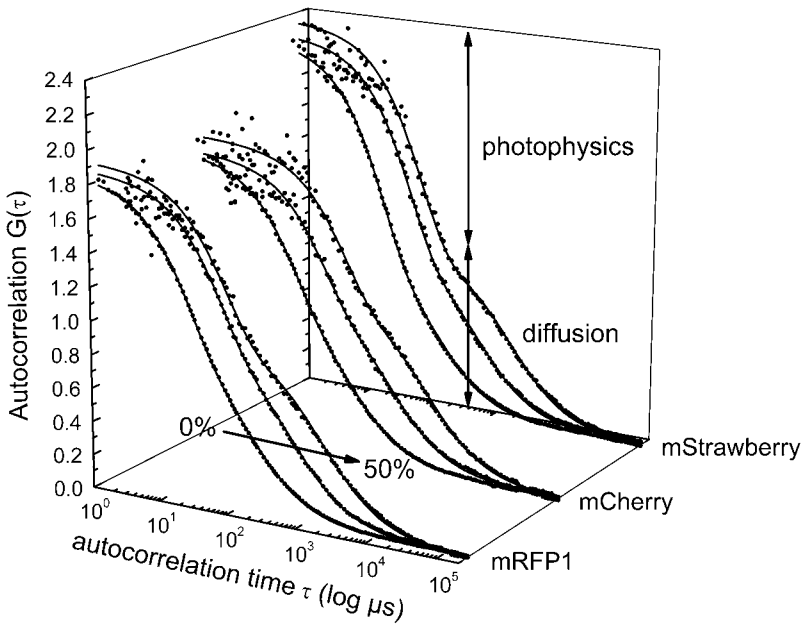

FIGURE 1 Experimental FCS curves of the mRFPs at $I_{exc} = 24$ kW/cm^2 normalized to the diffusional component. In each group of three curves, the concentration of glycerol was 0%, 25%, and 50% (v/v). From left to right: mRFP1, mCherry, and mStrawberry. The solid lines are global fits with Eq. 1, where the fraction of the flickering was linked within one set.

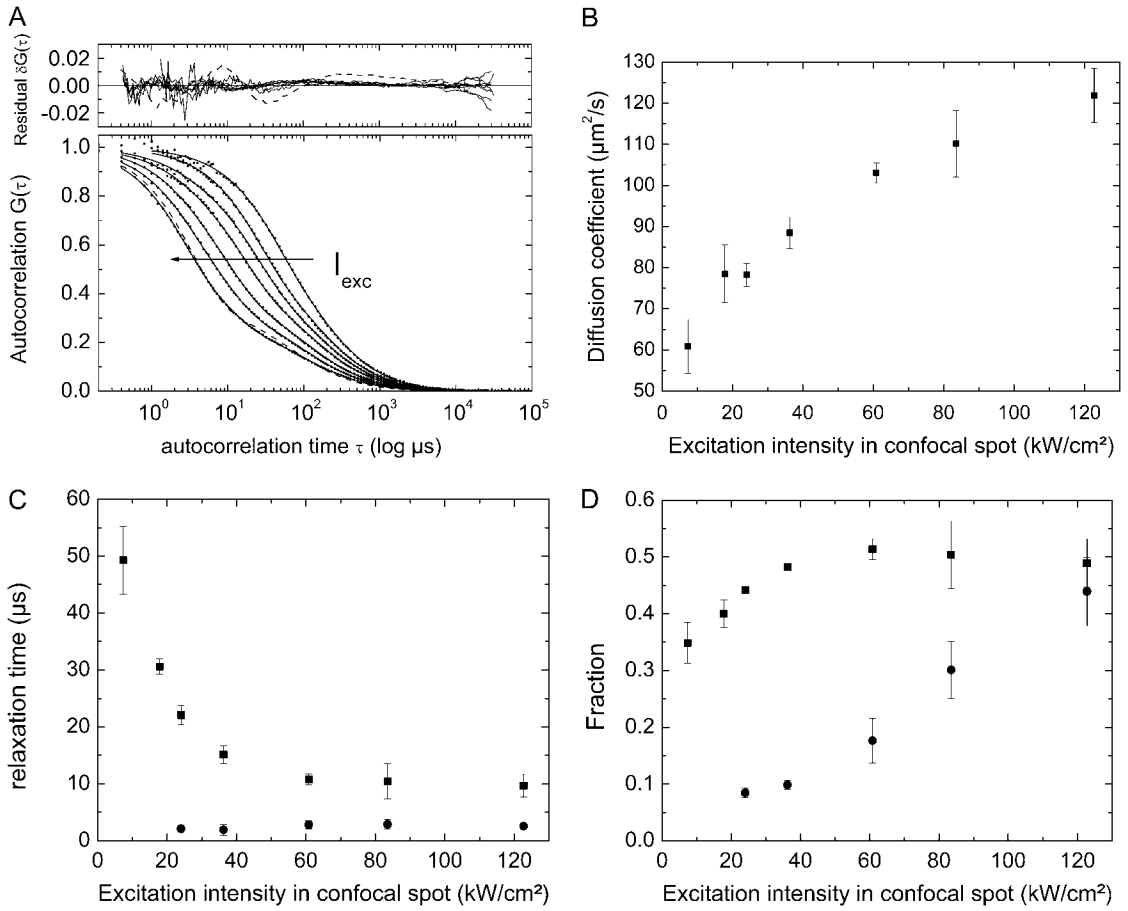

FIGURE 2 (*A*) Experimental autocorrelation curves of mRFP1 in aqueous buffer at excitation intensities ranging from (*right to left*) 2 to 122 kW/cm^2. The curves were normalized to $G(0) = [N \cdot (1 - F_1) \cdot (1 - F_2)]^{-1}$ to emphasize the effect of I_{exc} on the fast component of the curve. It is worth noting that normalization in this manner causes the $G_D(0)$ (Eq. 1) to decrease at increasing I_{exc}, even though the concentration stays constant. For the highest I_{exc}, both a one- (*solid line*) and two- (*dashed line*) exponential fit are shown. (*B*) Apparent diffusion coefficient after fitting with Eq. 1. (*C*) Relaxation times of the flickering (■) and triplet (●) processes. (*D*) Fraction of the fast processes when $G(0)$ is normalized to 1.

higher I_{exc} regimes, as has been already observed for other GFPs (25,29). These measurements thus suggest that there are (at least) two different dark states for mRFP1 When mCherry and mStrawberry were measured, a similar trend was observed (see Figs. S1 and S2 in Supplementary Material, Data S1).

Moreover, for all three mRFPs we found that for the slower flickering process the associated dark fraction does not tend to zero in the limit of zero excitation intensity (Fig. 2 *D*; see Figs. S1 *D* and S2 *D* in the Supplementary Material, Data S1). Therefore, we conclude that one of the two dark states observed with ensemble FCS is populated even in the absence of excitation light, but that its formation is accelerated through irradiation, whereas the other dark state is only occupied when excitation light is present.

pH Dependence

We explored the effect of varying pH values on the dark-state formation in mRFP1 and mFruits, because it has been shown for other fluorescent proteins that the pH can play a role in this process. FCS measurements of mRFP1 were performed at different values of pH in 50% (v/v) glycerol (see Materials and Methods) to allow for an easy visual inspection of the autocorrelation curves (Fig. 3 *A*). To emphasize the effect of the pH on the flickering dynamics, the autocorrelation curves were normalized with respect to the translational diffusion part. The fraction of mRFP1 molecules that is, on average, in a dark state shifted from 50% ± 1% to 64% ± 1% when going from pH 7 to 12, and the associated relaxation time shifted from 98.6 ± 3.0 μs to 112.3 ± 4.2 μs, indicating that mRFP1 is more often and longer in a dark state (because $1/\tau_{relaxation} = k_{relaxation} = k_{bright \rightarrow dark} + k_{dark \rightarrow bright}$). In mCherry and mStrawberry, a similar increase in the fraction and relaxation times were observed (see Fig. S3 *A* of the Supplementary Material, Data S1).

In an acidic environment (pH 5 and below), a different fast process appears in the autocorrelation curve (data not shown). This process has already been described for eGFP and likely represents the protonation equilibrium of the hydroxyl moiety of the modified Tyr66 residue in the chro-

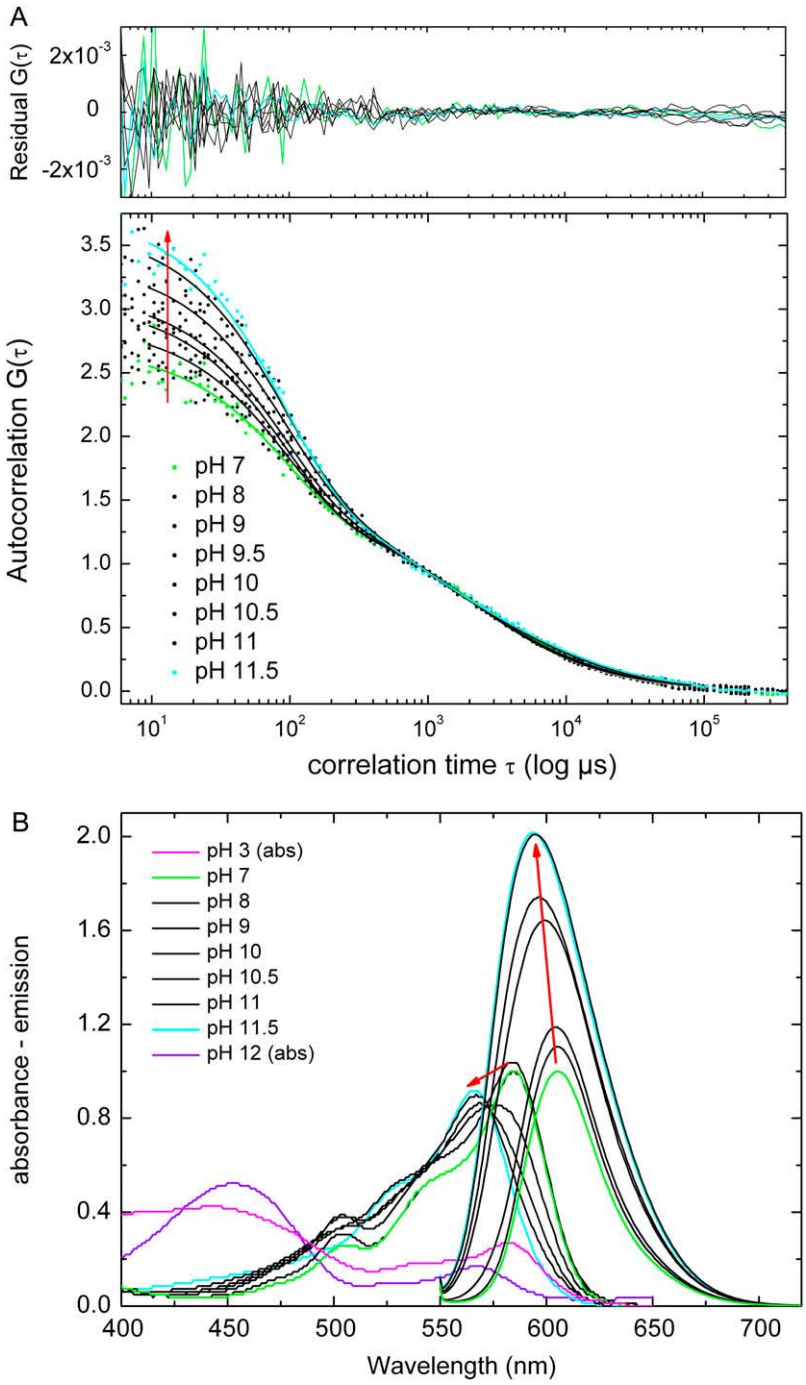

FIGURE 3 (*A*) Experimental autocorrelation curves of mRFP1 at $I_{exc} = 61$ kW/cm^2 in pH buffer supplemented with 50% (v/v) glycerol. The autocorrelation curves were normalized to the diffusional part of the curve. Normalization in this manner emphasizes the effect of pH on the flickering. The red arrow indicates the increase of the fraction of the flickering on increasing pH from 7 to 11.5. (*B*) Absorption and emission spectra of mRFP1 at varying pH values. The red arrow indicates the hypsochromic shift of the spectra and the increase of the quantum yield of mRFP1.

mophore (29). Because the chromophore is only fluorescent in the anionic state, protonation of Tyr66 at a low pH quenches the fluorescence, giving rise to a dark state in the autocorrelation curve. Interestingly, although DsRed shares the same chromophore as mRFP1, the dark states of DsRed are not pH-dependent (13).

To investigate if the effects observed in FCS are related to changes in the steady-state absorption and emission properties, the pH-dependence of mRFP1 absorption, emission, and excitation spectra were measured from pH 3 to 12 (Fig. 3 *B*). The absorption maximum of mRFP1 shifted from 584 to 567 nm when going from pH 7 to 11, which is in good agreement with measurements on mCherry (30). Below pH 7, the absorption spectrum did not change significantly. In the emission spectra, a similar blue shift from 605 to 595 nm was observed when increasing from pH 7 to 11 (Fig. 3 *B*). More interestingly, when raising the pH from 7 to 11, the intensity of fluorescence drastically increased ($I_{\lambda,max}$ increased by a factor ~2.4). The shift of the emission intensity with pH fitted well with a model for a monoprotic acid-base system

(see Fig. S3 *B* of the Supplementary Material, Data S1). In addition, a pKa of 9.9 ± 0.1 was obtained for the process, which is in close accordance with values reported on mCherry and mStrawberry (30). The apparent fluorescence quantum yield of the chromophore thus increases as a result of a different protonation state of the chromophore environment. This brightness increase cannot be due to a decrease in the fraction or relaxation time of the dark state, because our FCS data show that, at a high pH, the dark state lives longer and occurs more frequently. In contrast, these observations can be explained based on the crystallographic information about mRFPs at different pH values. For example, a significant drop of the twist and tilt angles of the chromophore was observed in mStrawberry when the pH was increased from 9.5 to 10.5 (30), in very good agreement with our observations on mRFP1. Chromophore coplanarity is a very important factor in the fluorescence efficiency of GFPs (as discussed further on in this article). Similar effects were seen in the excitation spectrum of mRFP1 (data not shown).

At pH 3 and 12 all fluorescence disappeared, indicating the denaturation of the protein. At these extreme pH values, the chromophore still showed a wide absorption peak in the blue (Fig. 3 *B*), as has been reported for other fluorescent proteins (19).

Single-molecule spectroscopy of immobilized mRFP1

We used single-molecule spectroscopy of immobilized mRFP1 to study the fast on-off dynamics without the contribution of diffusion. A typical single-molecule intensity trace of mRFP1 in a PVA matrix is shown in Fig. 4, *A* and *B*. Frequent on-off blinking is clearly observed in several timescales, even up to seconds, revealing a reversible transition from a bright to a dark state, similar to our observations in the FCS experiments. The flickering was found for the large majority of the molecules measured (>90%). In general, the emission intensity level is not stable due to this blinking, but there were no evident sequential photobleaching steps, which is consistent with the monomeric form of the protein. For comparison, immobilized DsRed showed several intensity levels as expected from its oligomeric form. In addition, on-off blinking also was present as reported previously (31–33), especially at the lower intensity levels after several units had been photobleached.

Autocorrelation curves of the fluorescence intensity of an immobilized molecule of mRFP1 could be typically fitted with three exponentials of timescales of hundreds of microseconds, a few milliseconds, and hundreds of milliseconds. Fig. 4 *C* shows an example with autocorrelation times of 540 μs, 1.8 ms, and 250 ms. The fastest of these processes might represent the flickering observed in the ensemble FCS measurements. The relaxation time found in the ensemble FCS measurements typically was <100 μs, but the difference might be attributed to the higher excitation intensity used in the ensemble FCS experiments. The slower processes might reflect protein conformational changes in a slower timescale (see Discussion).

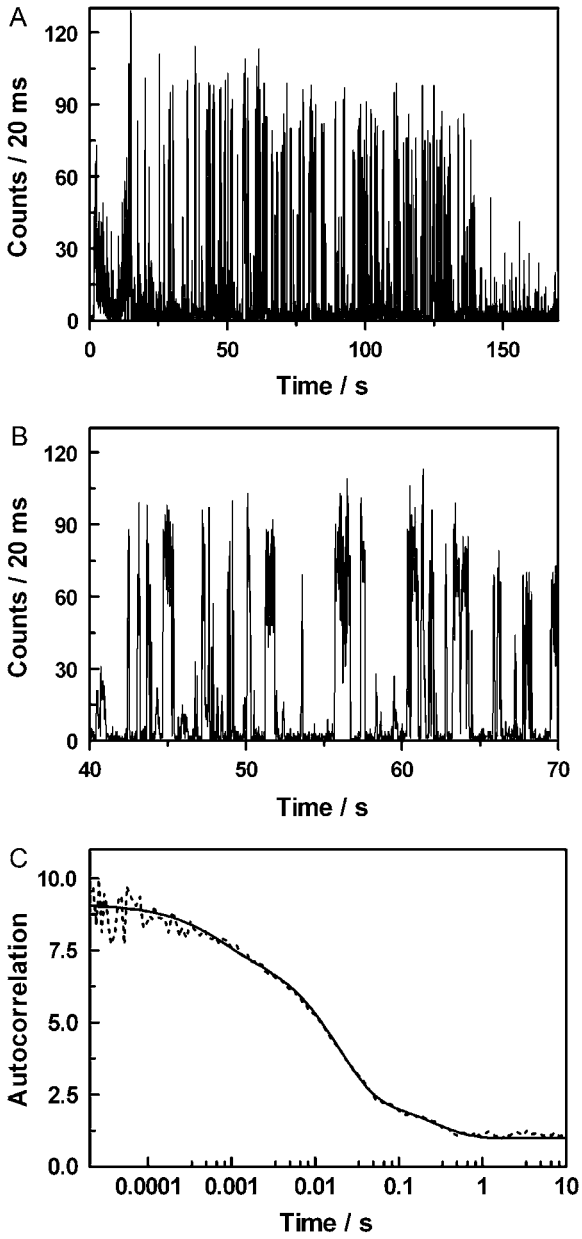

FIGURE 4 (*A*) Single-molecule fluorescence trajectories of mRFP1 immobilized in PVA matrix. (*B*) Magnified region from panel *A* (40–70 s). (*C*) Typical autocorrelation curve of an immobilized single-molecule and fit with a three-exponential function (540 μs, 1.8 ms, 250 ms).

The distribution of fluorescence lifetimes, analyzed in bins of 2000 photons, is quite broad but peaks at about the main value found in bulk experiments (1.8 ns; see next section).

Time-resolved fluorescence spectroscopy of mRFP1 and mFruits

We performed time-resolved fluorescence measurements on bulk solutions of mRFPs to gain more insight into their

excited-state dynamics. mRFP1 has main fluorescence decay of 1.8 ns (96%) and a small component of ~0.4 ns (4%) when excited at 543 nm and monitored at 610 nm (see Fig. S4 of the Supplementary Material, Data S1). A nonpure monoexponential decay for mRFP1 has been already reported in the literature (6). mStrawberry (see Fig. S4 of the Supplementary Material, Data S1) and mCherry (Fig. 5) also decayed biexponentially, the former with components of 2.1 ns (85%) and ~1 ns (15%) and the latter with 1.6 ns (90%) and ~0.7 ns (10%) (Fig. 5). The presence of multiexponential decays in GFPs could be associated with conformational changes (see Discussion). In contrast, DsRed decayed monoexponentially when excited at 543 nm (13,31). A multiexponential decay was found when excited at 470 nm due to energy transfer processes from the immature subunits of the tetramer, but this process cannot occur in the case of the monomer.

DISCUSSION

Dark states of mRFPs

mRFP1, mCherry, and mStrawberry all reveal a pH- and I_{exc}-dependent flickering, as shown in this work by means of FCS. As mentioned in the Introduction, light-induced flickering has been observed previously with FCS and single-molecule spectroscopy in RFPs such as DsRed and eqFP611 (4,14,15).

The conformation of the chromophore can have a large influence on the spectroscopic properties of a protein. Both *cis* conformations (DsRed and its variants) and *trans* conformations (eqFP611) around the methylene bridge between the two cyclic parts can be fluorescent. In addition, coplanarity of the hydroxyphenyl and the imidazolinone moieties of the chromophore seem to be indispensable for fluorescence (34,35). It has been suggested that conformational rearrangements of the chromophore might be responsible for flickering in these RFPs, because the timescales are consistent with these changes (15). In contrast, amino acids in close proximity of the chromophore can also affect the chromophore fluorescence. The pH-dependence of the mRFP1 fluorescence, as evidenced here, is most probably a consequence of an altered chromophore environment (see next section). Moreover, the looser H-bonding network in mRFP1 and mFruits compared to DsRed might contribute to the conformational freedom of the chromophore in the β-barrel (5).

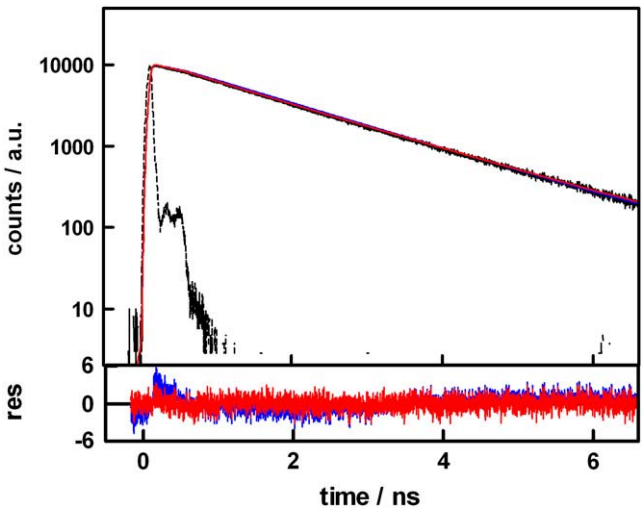

FIGURE 5 Fluorescence decay of mCherry (λ_{det} = 610 nm, *solid line*) and instrument response function (*dotted line*). Fit and residuals of a one-exponential function ($\chi^2 = 1.61$, *blue*) and a two-exponential function ($\chi^2 = 1.05$, *red*).

Our results for the time-resolved fluorescence experiments are consistent with conformational rearrangements of the chromophore in mRFP1 and mFruits. Similar biexponential decays in other RFPs, such as eqFP611 and HcRed, have been associated with the presence of two different conformers (17,27). Furthermore, we showed here, with FCS, that the conformers interconvert in the excited state, because the flickering is light-induced. In the case of DsRed, the pure monoexponential decay is a consequence of the reduced conformational mobility in the excited state.

As for the blinking of immobilized mRFP1, the fact that the flickering is slowed in the rigid PVA matrix would be consistent with the attribution of the process to a conformational change (27). It has been demonstrated previously that binding of eqFP611 to polyethylene glycol-covered glass surfaces did not affect the flickering rates compared to solution (15), although the latter process was suppressed when eqFP611 was deposited on bare glass. The PVA matrix used in our single-molecule experiments might be slightly more rigid than polyethylene glycol but still allows a certain conformational freedom. The slight effect of solvent viscosity on the flickering component observed in FCS is also consistent with the above (although viscosity will clearly have a greater effect on the diffusion component). In contrast, autocorrelation times in the tens of milliseconds timescale have been assigned previously to the interconversion between *cis* and *trans* conformations mediated by polymer motions in immobilized HcRed (27). A hybrid quantum mechanics/molecular dynamics study might be useful to reveal the mechanisms of *cis-trans* isomerization and/or loss of chromophore planarity that is responsible for the observed fluorescence flickering in mRFPs, as was done previously for GFP (36).

By comparing DsRed and eqFP611, the latter of which has been shown to have a smaller oligomerization tendency than the former (4), it was shown previously by Schenk et al. that oligomerization does not influence greatly the flickering dynamics observed with FCS (15), although the difference in oligomerization state between the two proteins in their experimental conditions is somewhat inconclusive. We have found with single-molecule FCS (see section ''Single-molecule spectroscopy of immobilized mRFP1'') that both immobilized mRFP1 and DsRed showed flickering, although the flickering was somewhat more frequent for DsRed in the lower-intensity levels, after several units had been pho-

tobleached. This situation would resemble that of mRFP1, although we cannot rule out the effect of the photobleached units of DsRed acting as ''traps''.

Structural basis for the pH-dependence of the mRFPs

It has been recently demonstrated that Glu-215 is the key residue responsible for the pH-induced spectral shift of mCherry and mStrawberry, as it is the only residue in the vicinity of the chromophore that markedly changes its conformation on an increase of the pH from 9.5 to 10.5 (Fig. 6 *A*) (30). Although such a pKa is very high for a Glu (the pKa for the γ-carboxyl group of Glu in solution is 4.3), there are reports in the literature of such high pKa values in some proteins (37) when the acid form is strongly stabilized. It is very intriguing that only the mRFPs show a pH-dependent red-shift and flickering, whereas all RFPs contain the same Glu-215 residue.

Fig. 6, *A* and *B*, show a stereo image of a 5 Å sphere around Glu-215 in mStrawberry and DsRed, respectively. Table 1 shows the residues surrounding Glu-215 that differ between DsRed and the mRFPs. The side chain of residue 41 is probably too distant from the side chain of Glu-215 to have an effect. Residues 42 and 44 are very similar among all RFPs. Residues 197 and 217 on the other hand differ strongly. Whereas these residues are hydrophobic in the mRFPs, they are polar and involved in H-bond formation in DsRed. From the crystal structure of DsRed, it is clear that Glu-215 forms a salt bridge with Lys-70 that is further stabilized by H-bridges with Ser-197 and Thr-217 (38). The deprotonated form of Glu-215 is thus strongly stabilized through the salt bridge causing a very low pKa of the carboxylic acid and providing an explanation for the lack of a pH-dependence of the fluorescence in DsRed.

In mStrawberry, however, the distance between the positively charged Lys-70 and the carboxylic acid oxygen of Glu-215 is increased to 5.72 Å, and the local environment becomes more hydrophobic due to the presence of the two hydrophobic residues Ile-197 and Ala-217. Lys-70 thus forms a salt bridge with Glu-148 and, moreover, a H-bond is formed between the protonated Glu-217 and the imidazolinone

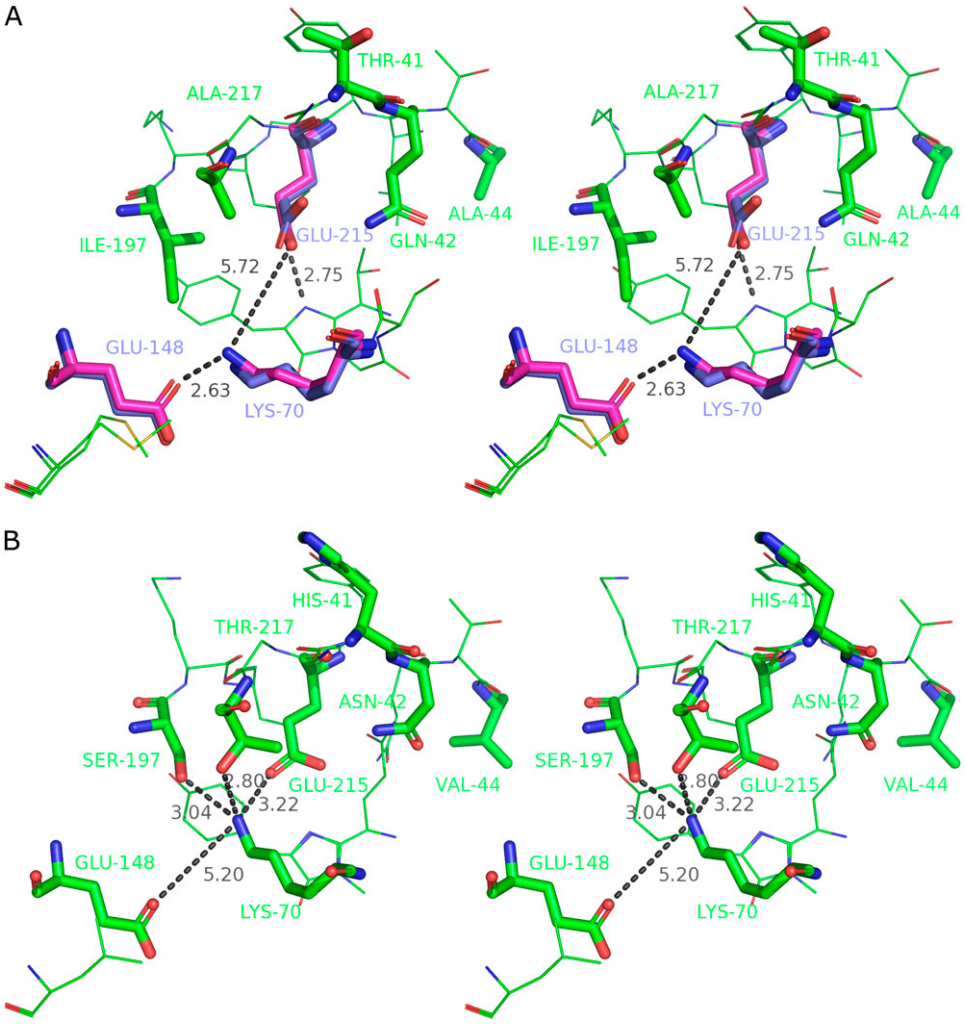

FIGURE 6 Ball and stick representation of the 5 Å-radius environment of Glu-215 in (*A*) mStrawberry and (*B*) DsRed. Residues that differ between mStrawberry and DsRed or have a markedly different conformation in acid or base are explicitly depicted as sticks. In mStrawberry, Lys-70, Glu-148, and Glu-215 are depicted pink in acid and blue in conjugated base conformation. H-bonds are depicted in gray, with the distance in angstroms. The figures were made with the PyMOL Molecular Graphics System (DeLano Scientific, Palo Alto, CA).

TABLE 1 Residues surrounding Glu-215 in RFPs that differ between DsRed and the mRFPs

Position	DsRed	mRFPs
41	His	Thr
42	Asn	Gln
44	Val	Ala
197	Ser	Ile
217	Thr	Ala

nitrogen of the chromophore. This explains the high pKa of Glu-215. By way of comparison, in eqFP611, residue 197 is a His and 217 is an Ala. From the crystal structure, it is apparent that there is an H-bond between His-197 and Glu-215 stabilizing the carboxylate form and explaining the lack of pH-dependence (4,14).

Our observed pH-dependence can now be explained in terms of this structural information. At a neutral pH, an H-bond between the chromophore and Glu-215 exists, which pulls the chromophore out of its planar conformation (30) causing a red shift of the spectrum and a decreased brightness. At a pH above the (high) pKa of Glu-215, the H-bond between the latter and the chromophore is broken and, as a result, the chromophore becomes more planar and so brighter. Due to the breakage of the H-bond, conformational rearrangements will be favored, and a more frequent dark state formation will occur. A similar pH-dependence has been recently observed in a related chromoprotein (39).

The transition pH for the mRFPs is also around the pKa of an ε-amino group of a Lys (10.5 in solution). In the acid and basic structures of the mRFPs, however, Lys-70 is forming a salt bridge with Glu-148, such that its deprotonation as a cause of the transition can be excluded. This interpretation is confirmed by the fact that Lys-70 in mStrawberry has only a slightly different conformation at pH 10.5 compared to pH 9.5.

Implications for cellular measurements

mRFPs are very promising for cellular measurements because they are spectrally well separated from the GFPs, and they are monomeric. Mocz has written a recent review on some interesting applications of the available fluorescent proteins (40). However, the appearance of flickering in the same timescale as diffusion (at the low I_{exc} necessary for in vivo measurements) can seriously complicate the analysis in FCS. To illustrate, we prepared a fusion protein of mRFP and eGFP, expressed it inside live human HeLaP4 cells, and performed FCS measurements, as described by De Rijck et al. (41). Because the fluorescence of the fused protein can be monitored in the green and the red channel simultaneously (with two-color excitation and detection), FCS analysis of mRFP1- and eGFP-fluorescence is possible. Table 2 summarizes the results after fitting the two autocorrelation curves to a model with one exponential and two diffusion components (the fast representing free diffusion and the slow representing hindered diffusion). It is clear that fitting of the mRFP1 autocorrelation curve gives a nonrealistic diffusion time for the freely diffusing protein (i.e., 39 μs for mRFPs versus 380 μs for eGFP), despite the fact that the flickering process is represented in the fitting. If the protein complex is bigger and diffusion is thus slowed down, then the processes can be separated well, as was the case in our in vitro viscosity measurements. If, on the other hand, the flickering of the mRFPs could be fastened or inhibited, their use in cellular measurements would be simplified considerably.

TABLE 2 Fit results for intracellular FCS on mRFP-eGFP

FCS channel		τ (μs)	Fraction (%)
eGFP	Free diffusion	380 ± 70	74.8 ± 13.6
	Hindered diffusion	16405 ± 2220	25.2 ± 13.6
	Photophysics (triplet)	4 ± 2	16 ± 2
mRFP1	Free diffusion	39 ± 17	65.5 ± 8.0
	Hindered diffusion	2481 ± 840	34.5 ± 8.0
	Photophysics (flickering)	63 ± 11	43 ± 7

Fitting was performed using a two-component diffusion model with one exponential. Goodness-of-fit was judged by looking at both the residual $\delta G(\tau)$ curve and the χ^2-value.

CONCLUSION

Fluorescence flickering in (m)RFPs seems to be a general behavior that might impair the analysis in FCS and FRET experiments. Unveiling the mechanism(s) responsible for this light-induced process may assist in the development of new and better mutants. In this work, we focused on the presence of this flickering in the monomeric RFPs mRFP1, mCherry, and mStrawberry and provide insight in the pH-dependence of the fluorescence flickering. Taking into account previous results on other RFPs, we offer a global picture of the structural basis of fluorescence flickering in (monomeric) RFPs. Further evolution of mRFPs should specifically address this problem, because we show that the implications in cellular measurements can be serious.

SUPPLEMENTARY MATERIAL

To view all of the supplementary files associated with this article, visit www.biophysj.org.

The authors thank Dr. Roger Y. Tsien (Howard Hughes Medical Institute-University of California at San Diego, La Jolla, CA) for providing the plasmids encoding the fluorescent proteins.

J. Hendrix was funded by a grant from the Institute for the Promotion of Innovation by Science and Technology in Flanders (IWT). P.D. was funded by a fellowship of the Fonds voor Wetenschappelijk Onderzoek (Aspirant van het FWO). Y.E. and J. Hofkens were funded by grants from FWO (G.0584.06 and G.0366.06, respectively). C.F. was funded by a postdoctoral fellowship of the KULeuven Research Fund (GOA 2006/2, Center of Excellence Institute for Nanoscale Physics and Chemistry, CREA2007). The Flemish Ministry of Education (ZWAP 04/007) is acknowledged by J. Hofkens and the Federal Science Policy of Belgium (IAP-VI/19) is acknowledged by Y.E.

REFERENCES

1. Shimomura, O. 2005. The discovery of aequorin and green fluorescent protein. *J. Microsc.* 217:1–15.
2. Prasher, D. C., V. K. Eckenrode, W. W. Ward, F. G. Prendergast, and M. J. Cormier. 1992. Primary structure of the Aequorea victoria green-fluorescent protein. *Gene.* 111:229–233.
3. Matz, M. V., A. F. Fradkov, Y. A. Labas, A. P. Savitsky, A. G. Zaraisky, M. L. Markelov, and S. A. Lukyanov. 1999. Fluorescent proteins from nonbioluminescent Anthozoa species. *Nat. Biotechnol.* 17:969–973.
4. Wiedenmann, J., A. Schenk, C. Rocker, A. Girod, K. D. Spindler, and G. U. Nienhaus. 2002. A far-red fluorescent protein with fast maturation and reduced oligomerization tendency from Entacmaea quadricolor (Anthozoa, Actinaria). *Proc. Natl. Acad. Sci. USA.* 99: 11646–11651.
5. Campbell, R. E., O. Tour, A. E. Palmer, P. A. Steinbach, G. S. Baird, D. A. Zacharias, and R. Y. Tsien. 2002. A monomeric red fluorescent protein. *Proc. Natl. Acad. Sci. USA.* 99:7877–7882.
6. Stepanenko, O. V., V. V. Verkhusha, V. I. Kazakov, M. M. Shavlovsky, I. M. Kuznetsova, V. N. Uversky, and K. K. Turoverov. 2004. Comparative studies on the structure and stability of fluorescent proteins EGFP, zFP506, mRFP1, ''dimer2'', and DsRed1. *Biochemistry.* 43:14913–14923.
7. Shaner, N. C., R. E. Campbell, P. A. Steinbach, B. N. Giepmans, A. E. Palmer, and R. Y. Tsien. 2004. Improved monomeric red, orange and yellow fluorescent proteins derived from Discosoma sp. red fluorescent protein. *Nat. Biotechnol.* 22:1567–1572.
8. Wang, L., W. C. Jackson, P. A. Steinbach, and R. Y. Tsien. 2004. Evolution of new nonantibody proteins via iterative somatic hypermutation. *Proc. Natl. Acad. Sci. USA.* 101:16745–16749.
9. Shaner, N. C., P. A. Steinbach, and R. Y. Tsien. 2005. A guide to choosing fluorescent proteins. *Nat. Methods.* 2:905–909.
10. Jach, G., M. Pesch, K. Richter, S. Frings, and J. F. Uhrig. 2006. An improved mRFP1 adds red to bimolecular fluorescence complementation. *Nat. Methods.* 3:597–600.
11. Merzlyak, E. M., J. Goedhart, D. Shcherbo, M. E. Bulina, A. S. Shcheglov, A. F. Fradkov, A. Gaintzeva, K. A. Lukyanov, S. Lukyanov, T. W. Gadella, and D. M. Chudakov. 2007. Bright monomeric red fluorescent protein with an extended fluorescence lifetime. *Nat. Methods.* 4:555–557.
12. Verkhusha, V. V., and A. Sorkin. 2005. Conversion of the monomeric red fluorescent protein into a photoactivatable probe. *Chem. Biol.* 12:279–285.
13. Heikal, A. A., S. T. Hess, G. S. Baird, R. Y. Tsien, and W. W. Webb. 2000. Molecular spectroscopy and dynamics of intrinsically fluorescent proteins: coral red (dsRed) and yellow (Citrine). *Proc. Natl. Acad. Sci. USA.* 97:11996–12001.
14. Malvezzi-Campeggi, F., M. Jahnz, K. G. Heinze, P. Dittrich, and P. Schwille. 2001. Light-induced flickering of DsRed provides evidence for distinct and interconvertible fluorescent states. *Biophys. J.* 81:1776–1785.
15. Schenk, A., S. Ivanchenko, C. Rocker, J. Wiedenmann, and G. U. Nienhaus. 2004. Photodynamics of red fluorescent proteins studied by fluorescence correlation spectroscopy. *Biophys. J.* 86:384–394.
16. Habuchi, S., M. Cotlet, T. Gensch, T. Bednarz, S. Haber-Pohlmeier, J. Rozenski, G. Dirix, J. Michiels, J. Vanderleyden, J. Heberle, F. C. De Schryver, and J. Hofkens. 2005. Evidence for the isomerization and decarboxylation in the photoconversion of the red fluorescent protein DsRed. *J. Am. Chem. Soc.* 127:8977–8984.
17. Loos, D. C., S. Habuchi, C. Flors, J. I. Hotta, J. R. Wiedenmann, G. U. Nienhaus, and J. Hofkens. 2006. Photoconversion in the red fluorescent protein from the sea anemone Entacmaea quadricolor: is cis-trans isomerization involved? *J. Am. Chem. Soc.* 128:6270–6271.
18. Schwille, P., S. Kummer, A. A. Heikal, W. E. Moerner, and W. W. Webb. 2000. Fluorescence correlation spectroscopy reveals fast optical excitation-driven intramolecular dynamics of yellow fluorescent proteins. *Proc. Natl. Acad. Sci. USA.* 97:151–156.
19. Gross, L. A., G. S. Baird, R. C. Hoffman, K. K. Baldridge, and R. Y. Tsien. 2000. The structure of the chromophore within DsRed, a red fluorescent protein from coral. *Proc. Natl. Acad. Sci. USA.* 97:11990–11995.
20. Reference deleted in proof.
21. Vosch, T., M. Cotlet, J. Hofkens, K. Van der Biest, M. Lor, K. Weston, P. Tinnefeld, M. Sauer, L. Latterini, K. Mullen, and F. C. De Schryver. 2003. Probing Forster type energy pathways in a first generation rigid dendrimer bearing two perylene imide chromophores. *J. Phys. Chem. A.* 107:6920–6931.
22. Maus, M., E. Rousseau, M. Cotlet, G. Schweitzer, J. Hofkens, M. Van der Auweraer, F. C. De Schryver, and A. Krueger. 2001. New picosecond laser system for easy tunability over the whole ultraviolet/visible/near infrared wavelength range based on flexible harmonic generation and optical parametric oscillation. *Rev. Sci. Instrum.* 72:36–40.
23. Enderlein, J., I. Gregor, D. Patra, T. Dertinger, and U. B. Kaupp. 2005. Performance of fluorescence correlation spectroscopy for measuring diffusion and concentration. *ChemPhysChem.* 6:2324–2336.
24. Dertinger, T., V. Pacheco, I. von der Hocht, R. Hartmann, I. Gregor, and J. Enderlein. 2007. Two-focus fluorescence correlation spectroscopy: a new tool for accurate and absolute diffusion measurements. *ChemPhysChem.* 8:433–443.
25. Widengren, J., U. Mets, and R. Rigler. 1999. Photodynamic properties of green fluorescent proteins investigated by fluorescence correlation spectroscopy. *Chem. Phys.* 250:171–186.
26. Jung, G., J. Wiehler, and A. Zumbusch. 2005. The photophysics of green fluorescent protein: Influence of the key amino acids at positions 65, 203, and 222. *Biophys. J.* 88:1932–1947.
27. Cotlet, M., S. Habuchi, J. E. Whitier, J. H. Werner, F. C. De Schryver, J. Hofkens, and P. M. Goodwin. 2006. Single molecule spectroscopic characterization of a far-red fluorescent protein (HcRed) from the Anthozoa coral *Heteractis crispa*. *Proc. SPIE.* 6098:609804–609811.
28. Jiménez-Banzo, A., S. Nonell, J. Hofkens, and C. Flors. 2008. Singlet oxygen photosensitization by EGFP and its chromophore HBDI. *Biophys. J.* 94:168–172.
29. Haupts, U., S. Maiti, P. Schwille, and W. W. Webb. 1998. Dynamics of fluorescence fluctuations in green fluorescent protein observed by fluorescence correlation spectroscopy. *Proc. Natl. Acad. Sci. USA.* 95:13573–13578.
30. Shu, X., N. C. Shaner, C. A. Yarbrough, R. Y. Tsien, and S. J. Remington. 2006. Novel chromophores and buried charges control color in mFruits. *Biochemistry.* 45:9639–9647.
31. Cotlet, M., J. Hofkens, S. Habuchi, G. Dirix, M. Van Guyse, J. Michiels, J. Vanderleyden, and F. C. De Schryver. 2001. Identification of different emitting species in the red fluorescent protein DsRed by means of ensemble and single-molecule spectroscopy. *Proc. Natl. Acad. Sci. USA.* 98:14398–14403.
32. Cotlet, M., J. Hofkens, F. Kohn, J. Michiels, G. Dirix, M. Van Guyse, J. Vanderleyden, and F. C. De Schryver. 2001. Collective effects in individual oligomers of the red fluorescent coral protein DsRed. *Chem. Phys. Lett.* 336:415–423.
33. Garcia-Parajo, M. F., M. Koopman, E. M. van Dijk, V. Subramaniam, and N. F. van Hulst. 2001. The nature of fluorescence emission in the red fluorescent protein DsRed, revealed by single-molecule detection. *Proc. Natl. Acad. Sci. USA.* 98:14392–14397.
34. Prescott, M., M. Ling, T. Beddoe, A. J. Oakley, S. Dove, O. Hoegh-Guldberg, R. J. Devenish, and J. Rossjohn. 2003. The 2.2 A crystal structure of a pocilloporin pigment reveals a nonplanar chromophore conformation. *Structure.* 11:275–284.
35. Henderson, J. N., and S. J. Remington. 2006. The kindling fluorescent protein: a transient photoswitchable marker. *Physiology (Bethesda).* 21:162–170.
36. Weber, W., V. Helms, J. A. McCammon, and P. W. Langhoff. 1999. Shedding light on the dark and weakly fluorescent states of green fluorescent proteins. *Proc. Natl. Acad. Sci. USA.* 96:6177–6182.

37. Forsyth, W. R., J. M. Antosiewicz, and A. D. Robertson. 2002. Empirical relationships between protein structure and carboxyl pKa values in proteins. *Proteins.* 48:388–403.

38. Yarbrough, D., R. M. Wachter, K. Kallio, M. V. Matz, and S. J. Remington. 2001. Refined crystal structure of DsRed, a red fluorescent protein from coral, at 2.0-A resolution. *Proc. Natl. Acad. Sci. USA.* 98:462–467.

39. Battad, J. M., P. G. Wilmann, S. Olsen, E. Byres, S. C. Smith, S. G. Dove, K. N. Turcic, R. J. Devenish, J. Rossjohn, and M. Prescott. 2007. A structural basis for the pH-dependent increase in fluorescence efficiency of chromoproteins. *J. Mol. Biol.* 368:998–1010.

40. Mocz, G. 2007. Fluorescent proteins and their use in marine biosciences, biotechnology, and proteomics. *Mar. Biotechnol. (NY).* 9:305–328.

41. De Rijck, J., L. Vandekerckhove, R. Gijsbers, A. Hombrouck, J. Hendrix, J. Vercammen, Y. Engelborghs, F. Christ, and Z. Debyser. 2006. Overexpression of the lens epithelium-derived growth factor/p75 integrase binding domain inhibits human immunodeficiency virus replication. *J. Virol.* 80:11498–11509.